CBPF-NF-078/96

A Model for Domain and Domain Wall NMR Signals in Magnetic Materials*

I.S. Oliveira and A.P. Guimarães

Centro Brasileiro de Pesquisas Físicas

Rua Dr. Xavier Sigaud, 150, Rio de Janeiro - 22290-180, Brazil

Abstract

Spin echo NMR signals in magnetic materials (simple metals, alloys or intermetallic compounds) generally result from mixed contributions of distinct magnetic regions of the sample, the magnetic domains and the domain walls. The amplitude of the signal is proportional to the so-called *enhancement factor* which in most of the cases greatly differs in these two regions, depending upon the wall mobility, the magnetic anisotropy, etc. The experimental access to domain and domain walls is possible, in principle, by a careful control of the RF power applied to the sample. In this paper a simple superposition model is proposed which includes both contributions to the NMR signal. We calculate the amplitude of the spin echo in magnetic powder samples and compare with experimental situations where it has been possible to separate different contributions to the signal. This has been done in some RCo_2 magnetic rare earth intermetallic compounds by analyzing the spectral linewidths and the curve of the spin echo amplitude vs. the applied RF field. Despite its simplicity, the present model allows the understanding of the main features of the NMR spectra and the dependence of the echo amplitude with the RF power in these compounds.

*Accepted in J. Mag. Mag. Mat.

1 Introduction

The technique of Spin Echo pulse NMR has been largely applied to the study of magnetic properties of metals and intermetallic compounds. From the magnetic nuclear spectra we can derive conclusions concerning directions of magnetization, transferred hyperfine fields, local moments on impurity sites, etc., whereas from the measurement of the spin-spin, spin-lattice relaxation times and the Knight-shift, information can be gained about the dynamic processes of interaction between the paramagnetic nuclear system and the lattice, the conduction electrons susceptibility, etc. [1, 2]. Less exploited is the ability of NMR to study the domain walls mobility, local anisotropy and the origin of the NMR signals through the dependence of the spin echo amplitude signal, and NMR spectra, upon the RF power level.

In general, a NMR spectrum in a ferromagnetic system will be composed of a mixture of signals coming from domains and domain walls. The proportion each of these regions will contribute to the final amplitude of the spin echo will depend on certain parameters such as the wall mobility, the wall width, the local anisotropy, the exchange energy, the relative volumes of domain and domain walls, and so on. The NMR signals appear augmented in a magnetic material, and these magnetic properties of the material will shape the so-called *enhancement factor* η. It is usual to separate this quantity into the domain and domain wall enhancement factors, η_D and η_W, respectively. Typical values for η_W are between 500 to 10000, whereas η_D usually ranges from 10 to 100 [1]. In a domain η_D can be estimated from the relation $\eta_D \approx B_{hf}/(B_a + B_o)$, where B_{hf} and B_a are the hyperfine and the anisotropy fields, respectively, and B_o the applied field [2].

Inside a domain wall, the amplification factor assumes a more complex form. As shown in ref [1], $\eta_W(x) \propto d\theta(x)/dx$, where $\theta(x)$ is the angle the magnetic moment at the position x inside the wall makes with the easy direction of magnetization in the domain. We should then, in principle, expect different amplification factors in different types of walls. For the particular case of a 180^o domain wall contained on a plane (such as in metallic iron) it can be shown that the amplification factor in the wall takes the simple form $\eta_W(x) = \eta_{oW} sech(x)$, where x measures the position of the magnetic ion in the wall from its center and η_{oW} is the enhancement factor at the center of the wall [3].

The enhancement factor amplifies the applied RF pulses, and also the returning NMR signal, and the fact that it is larger inside the domain walls may lead to ambiguous

interpretation of NMR data, as pointed by Dormann [4]. In fact, depending on particular experimental parameters, such as the available RF power level, the response of the resonant circuit, etc., significant variation in the linewidth, frequency shifts, etc., may occur.

A model for the spin echo amplitude from domain walls in magnetic powders was proposed a long time ago by M.B. Stearns (see below) [7]. In this paper we propose a simple superposition model to include both contributions from pure domains and domain walls to the NMR signal in magnetic samples, and compare with experimental results of spectroscopy and dependence of the spin echo amplitude with the RF power level in $GdCo_2$, $TbCo_2$ and $DyCo_2$. The series RCo_2 (R = rare earth) is particularly suited to the purpose of the present investigation since the magnetic anisotropy, walls width, etc., can be easily changed by the adequate choice of the rare earth.

2 Model Description

The dependence of the amplitude of the spin echo signal upon the RF intensity in a ferromagnetic sample can be derived from the basic expressions for the transverse components of the nuclear magnetization appearing after a sequence of two RF pulses with durations τ_a and τ_b separated by a time interval equal to $\Delta\tau$. At $t = 2\Delta\tau$ [5, 6]:

$$m_x = 2m_o sin^3\theta cos\theta sin^2\left(\frac{b\tau_a}{2}\right) sin^2\left(\frac{b\tau_b}{2}\right)$$

$$m_y = m_o sin^3\theta sin(b\tau_a) sin^2\left(\frac{b\tau_b}{2}\right) \tag{1}$$

where $\gamma_n b = (\Delta\omega^2 + \omega_1^2)^{1/2}$ is γ_n times the effective field in the rotating frame, $\theta = atan(\omega_1/\Delta\omega)$, $\Delta\omega = \omega - \gamma_n B_{hf}$, $\omega_1 = \gamma_n B_1$. m_o is the nuclear equilibrium magnetization, B_{hf} the hyperfine field and B_1 the amplitude of the RF field.

The spin echo amplitude, defined as $\epsilon \equiv (m_x^2 + m_y^2)^{1/2}$, will be, at resonance ($\Delta\omega = 0$), for a pair of pulses with the same duration $\tau_a = \tau_b = \tau$, equal to

$$\epsilon(B_1) = m_o sin(\gamma_n B_1 \tau) sin^2\left(\frac{\gamma_n B_1 \tau}{2}\right) \tag{2}$$

The above expression represents the signal amplitude in a non-magnetically ordered material, such as water or glycerin. In ferromagnetic powdered samples a number of

peculiarities have to be taken into account to the problem, among these the fact that in these materials the enhancement factor differs in domain and domain walls.

In 1967 M.B. Stearns worked a model out to explain the main features of domain wall NMR spectra in powdered ferromagnetic samples, and successfuly applied it to the case of iron metal [7]. At the resonance, the spin echo amplitude for a pair of RF pulses with the same width τ will depend on the RF field amplitude B_1 according to:

$$\epsilon_W(B_1) = m_o\eta_{oW}\int_0^\infty\int_0^1 sin^2\frac{1}{2}(\alpha_o z sechx)sin(\alpha_o z sechx)zsechxp(z)dzdx \qquad (3)$$

where $\alpha_o = \gamma_n\eta_{oW}B_1\tau$. The function $p(z)$ is related to the distribution of the areas of the walls [7]. Thus, for a given product $B_1\tau$, we can extract η_{oW} from a curve $\epsilon(B_1)$ vs. B_1. The larger the product $\gamma_n\eta_{oW}$ (for $B_1\tau$ fixed) the smaller will be the RF power necessary to reach the maximum of the curve. Figure 1 shows an example obtained for the ^{57}Fe NMR in metallic iron with $\tau = 0.5\mu s$. The horizontal axis is ploted as B_1/B_{1max}, where $B_{1max} \approx 10$ Gauss. The continuous line represents curve (3) with $\eta_{oW} \approx 6200$, which agrees with the value given in ref [7]. We observed that the shape of the curve is not very sensitive to the actual form of the function $\eta(x)$, as long as it remains even in the variable x.

In order to include the contribution from pure domains, we start from expressions (1), for the components of the spin echo. Let φ be the angle between the direction of the domain magnetization and the RF field $\mathbf{B}_1$. The component of the field perpendicular to the nuclear magnetization is then $B_1 sin\varphi$. So the argument of the *sin* functions in expression (2) must be replaced by $x = \gamma_n\eta_D B_1\tau sin\varphi$. Now, following Stearns argument [7] the detected signal is multiplied by the same factor $\eta_D sin\varphi$. Integrating over $d(sin\varphi) = cos\varphi d\varphi$ between $\varphi = \pm\pi/2$, one obtains at resonance:

$$\epsilon_D(B_1) = m_o\eta_D\int_{-\pi/2}^{+\pi/2} sin(\gamma_n\eta_D B_1\tau sin\varphi)sin^2\left(\frac{\gamma_n\eta_D B_1\tau sin\varphi}{2}\right)cos\varphi sin\varphi d\varphi$$

$$= \frac{\eta_D m_o}{\alpha^2}\int_{-\alpha}^{+\alpha} xsinxsin^2\left(\frac{x}{2}\right)dx$$

$$= \frac{\eta_D m_o}{\alpha^2}\left[sin\alpha - \frac{1}{8}sin(2\alpha) - \alpha cos\alpha + \frac{1}{4}\alpha cos(2\alpha)\right] \qquad (4)$$

where $\alpha = \gamma_n\eta_D B_1\tau$. Figure 2 shows the effect of averaging over the directions of the RF field by comparing expressions (2) and (4) for $\eta_D = 1$. Note from this result that for small values of B_1, $\epsilon \propto B_1$, contrary to expression (2), where $\epsilon \propto B_1^3$

In our model, the resulting NMR signal will be given by

$$\epsilon(B_1) = C_W \epsilon_W(B_1) + C_D \epsilon_D(B_1) \tag{5}$$

where $C_W = m_o \eta_{oW} V_W$ and $C_D = m_o \eta_D V_D$ are the relative contributions from the walls and the domains, respectively. V_D and V_W represent the fractions of the domain and domain wall volumes which effectively contribute to the signal.

In the following sections we compare the experimental results on RCo_2 compounds with the above expression. The model does not take into accound various effects which are usually present in the NMR of magnetically ordered compounds. Nevertheless, we will see that the main aspects of the experimental results can be understood, in particular those for $DyCo_2$ and $GdCo_2$. The limitations of expression (5) are discussed at the end of the concluding section.

3 Experimental Details

The compounds were prepared from pure elements melted in an arc-furnace under Argon atmosphere, and annealed to minimize lattice deffects. The samples were powdered and immersed in silicone oil to prevent noise from grain vibrations at 4.2 K. For the curve of figure 1 we used iron powder supplied by Goodfellow, with purity 99% and maximum grain size of 60 μm. A cylindrically shaped plastic sample holder with approximate volume 2 cm^3 was filled with the sample and inserted into a coil, built according to ref. [8], soldered at the end of a 50 Ω coaxial cable. The spin echo amplitude and spectra were measured in an automatic pulse NMR spectrometer. The conditions of excitation were: pulse widths, $\tau_a = \tau_b = \tau = 0.5 \mu s$ for $GdCo_2$ and $TbCo_2$; for $DyCo_2$ we set $\tau = 2.0 \mu s$. Pulse separation equal to $\Delta\tau = 60 \mu s$ and repetition rate 0.1 kHz. The signal was detected in quadrature and possible differences in the gain of the two components of the spin echo at the output of the "audio" amplifier were corrected by swapping the amplifier input channels and taking the appropriate average to build the final signal [9]. The RF power was controlled by a variable 60 dB power attenuator at the output of the RF power amplifier, a broadband ENI model 3100LA, 100 Watts. The value of $B_1/B_{1max} = 1$ corresponds to 0 dB of attenuation. The measurements were all taken at liquid helium temperature, 4.2 K.

4 Results and Discussion

Figure 3 shows the NMR spectra of ^{59}Co in $GdCo_2$, $DyCo_2$ and $TbCo_2$ at 4.2 K and low RF power level. The continuous lines represent Lorentzian fits from which we extracted the parameters shown in table I. Figure 4 shows the same set of spectra for maximum RF power ($B_1/B_{1max} = 1$); the respective fitted parameters are also shown in table I. These spectra are in good agreement with ref. [10]. The two lines appearing in the spectra of $TbCo_2$ are attributed to the existence of two magnetically inequivalent sites which we shall label site I (lower frequency) and site II (higher frequency). We note from the table that the NMR frequencies do not change appreciably with the RF power in Gd and Dy compounds. In $TbCo_2$ a shift of about 1 MHz in the first line and 2 MHz in the second line occurs. Also, the linewidths for $DyCo_2$ and $TbCo_2$ are not much affected. However, increasing the power practically halves the linewidth of $GdCo_2$. These features exemplify what was said at the introduction of this paper about changes in NMR spectra of magnetic materials upon the RF power. We can try now to correlate these results with the curve of RF power in these compounds and compare with equation (5).

Figure 5 shows the ϵ vs. B_1/B_{1max} curves for the three compounds. The measurements were taken at the central frequencies of each spectrum, the excitation conditions as described in the previous paragraph, except that for $DyCo_2$ we set $\tau = 6\mu s$. The differences in their behavior are very clear. In $TbCo_2$ the measurements were taken at the two magnetic sites; both curves resemble that for metallic iron (figure 1) and are assigned to pure domain walls. Here we obtained a value of η_{oW} in site I which is about half of that in site II. It is not of our knowledge any published report where a similar situation has been observed. One possible explanation could be difference in the local anisotropies at the two sites. We found that a better adjustment of the theoretical curve to the experimental data at higher values of B_1/B_{1max} could be achieved in both lines if we superimposed another curve with $\eta_{oW} = 1350$ in site I and $\eta_{oW} = 1450$ in site II. According to ref. [11, 12], this behavior could in principle be ascribed to the excitation of nuclei in the domain wall edges for large values of B_1/B_{1max}. In this case we would have the same wall "labeled" by two different values of η_W: one for its center, and another for the edges. Another possibility would be to consider contributions from "70^o" walls, those contained on the plane
$[111] \rightarrow [11\overline{1}]$, etc., with a smaller amplification factor. On the basis of the present data

we cannot decide between these two possibilities, but we think two types of walls must exist in these compounds, and we keep the second interpretation. In figure 5, broken lines represent individual contributions to the final signal amplitude, whereas full lines represent equation (5).

$DyCo_2$ exhibits a situation where the maximum of the curve could just be reached for the available maximum RF power. In this figure the continuous line represents equation (4) with $\eta_D = 8$.

$GdCo_2$ shows an intermediate case, where we can distinguish two regions: that for $B_1/B_{1max} \leq 0.4$ corresponding to signals from the domain walls, whereas above this value the NMR signal originates from the domains. The broken lines in the figure represent the separate contributions to the signal. Here again a better agreement between theory and experiment is achieved if we consider another curve with $\eta_{oW} = 500$, corresponding, e.g., to 90^0 domain walls ([100] $\rightarrow$ [010], etc.).

We can estimate the anisotropy fields in $GdCo_2$ and $DyCo_2$ using the relation $B_a \approx 2\pi\nu_o/\eta_D\gamma_n$, [2]. Here ν_o is the NMR central frequency. By replacing values from table I we find $B_a = 0.6$ kGauss for $GdCo_2$ and 8.2 kGauss for $DyCo_2$, which are of the right order of magnitude [2, 11].

The above picture is consistent with the NMR spectral data: we should expect broader resonance lines inside the walls, since the inhomogeneity in the local field is larger in this region. The linewidths of $DyCo_2$ (at both power levels) and $GdCo_2$ at maximum RF power are practically the same (see table I). This fact associated with the curves of figure 5 allows us to interpret the NMR signals in $DyCo_2$ as originating purely from the magnetic domains.

5 Conclusions

In this paper we propose a simple superposition model based on Stearns model [7] to the NMR signal intensities in magnetic samples including domain and domain walls contributions. The amplitude of the signals from domains and domain walls is proportional to the product of the respective enhancement factor by the effective volumes in the sample which are accessed by the RF field. We obtained general agreement between the model and the experimental data in RCo_2 compounds, where the characterization of the signal

by the dependence of the spin echo amplitude upon the RF power was followed by an analysis of their spectral linewidths.

The complex dependence of the ^{59}Co NMR in $TbCo_2$ upon the RF power level has been observed by other authors [10]. The origin of the frequency shift in the NMR spectra of this compound is still unclear. A similar behavior is present in the NMR spectra of other Laves phase compounds, namely ^{27}Al in $GdAl_2$ [13] and ^{59}Co in $HoCo_2$ [14] both presenting two resonance lines.

The relatively small NMR signal in $DyCo_2$ is due to its low amplification factor in the domains, derived from a large magnetic anisotropy. This compound is likely to have narrow domain walls, decreasing appreciably the parameter C_W in equation (5). This interpretation is consistent with the fact that among the three compounds studied in this paper, $DyCo_2$ is the only one where no significant changes, either in the line position or in the linewidth of the spectra, are observed as a function of the RF power.

$GdCo_2$ is the case where the mixture of domain and domain wall signals becomes more apparent. Also in this case, contributions from two types of domain walls (180^o and 90^o) seem to exist. The dramatic narrowing of the ^{59}Co NMR spectrum upon the increase of the RF power level supports the picture given here.

The above model is oversimplified in some aspects, for it does not take into account various effects which are inherent to the NMR of magnetic metals. Among these we can list the quadrupolar interaction, the skin effect and the dependence of the spin-spin relaxation time T_2 with the position of the nucleus within the wall. Also, a simple superposition of the signals (equation 5) does not consider the shielding of the RF field in the domains, caused by the motion of domain walls. Stearns expression for domain wall signals is based upon Bloch equations, which in turn are classical equations of motion and do not contain quadrupolar interaction effects. The skin effect and the dependence of T_2 with the position of the nucleus within the wall would imply two more integrals in (3) and one more in (4). Kotzur et al. [15] analyzed the influence of the skin effect in the spin echo amplitude of non-magnetic metals. Their model, obtained from a quantum-mechanical approach, agrees with experimental results in nickel foils of different thickness, mainly for low values of the rotation angle. Although the various effects typical to magnetically ordered materials are absent in their case (enhancement factor, shielding by domain walls motion, etc.) the shape of curves ε vs. rotation angle, for small values of the rotation

angle, are similar to that obtained for pure domain signals in the present paper.

It is not clear how the shielding effect should be included in expression (5), but this effect is decreased in a real crystal, since the motion of the walls is always hindered by defects and impurities, making the shielding not perfect.

Whereas the above might be true and it is worth considering, it seems that Stearns model picked the main aspects of the problem. She applied the model to iron powder. ^{57}Fe has spin $I = 1/2$ and consequently zero electric quadrupole interaction. Now, ^{59}Co has $I = 7/2$ and $Q \approx 0.5 \times 10^{-28} m^2$ and the quadrupolar interaction in present. However, on almost every case the splitting is smaller than the linewidth. A "Stearns model" including quadrupolar interaction and the other effects mentioned above seems to be very appealing, although we can still observe *qualitative* agreement between the original expression and the experimental results. The basic aim of the present paper is to show that despite its simplicity, a simple superposition model can help to understand the changes in the NMR spectra in ferromagnetic powders upon the RF intensity.

Table I

Compound	ν_o(MHz)	$\Delta\nu$(MHz)	B_1/B_{1max}	η
$GdCo_2$	61.64(7)	1.2(2)	1.0	$\eta_D = 95$
	61.75(9)	2.32(3)	0.1	$\eta_{oW}^{(180)} = 2000$
				$\eta_{oW}^{(90)} = 500$
$TbCo_2$	51.39(9)	7.5(4)	0.1	$\eta_{oW}^{(I,180)} = 1800$
	61.51(3)	5.5(2)		$\eta_{oW}^{(II,180)} = 3500$
				$\eta_{oW}^{(I,50)} = 1350$
				$\eta_{oW}^{(II,50)} = 1450$
	52.5(3)	6(1)	1.0	
	63.53(7)	4.5(2)		
$DyCo_2$	65.80(1)	1.13(3)	1.0	$\eta_D = 8$
	65.85(1)	1.06(4)	0.6	

Figure Captions

Figure 1 - Dependence of the spin echo amplitude signal upon the RF power level in powdered metallic iron. The continuous line represents equation (3) for $\eta_{oW} = 6200$ (see text).

Figure 2 - Effect of averaging over the directions of the RF field in respect to the hyperfine field. The broken line represents equation (2); the continuous one, equation (4).

Figure 3 - ^{59}Co NMR spectra in $GdCo_2$, $DyCo_2$ and $TbCo_2$ at low values of the RF power, taken at 4.2 K. The continuous lines represent Lorentzian fits from which we extracted the positions and linewidths of the spectra shown in table I.

Figure 4 - ^{59}Co NMR spectra in $GdCo_2$, $DyCo_2$ and $TbCo_2$ at high values of the RF power, taken at 4.2 K. The continuous lines represent Lorentzian fits from which we extracted the positions and linewidths of the spectra shown in table I.

Figure 5 - Dependence of the spin echo amplitude upon the RF power level in $GdCo_2$, $DyCo_2$ and $TbCo_2$ at 4.2 K. The broken lines represent different contributions from domain and domain walls to the signals, and the continuous lines represent the calculated signals from equation (5).

Table Caption - ^{59}Co NMR line positions, linewidths and enhancement factors for domain and domain walls in RCo_2 compounds at 4.2 K.

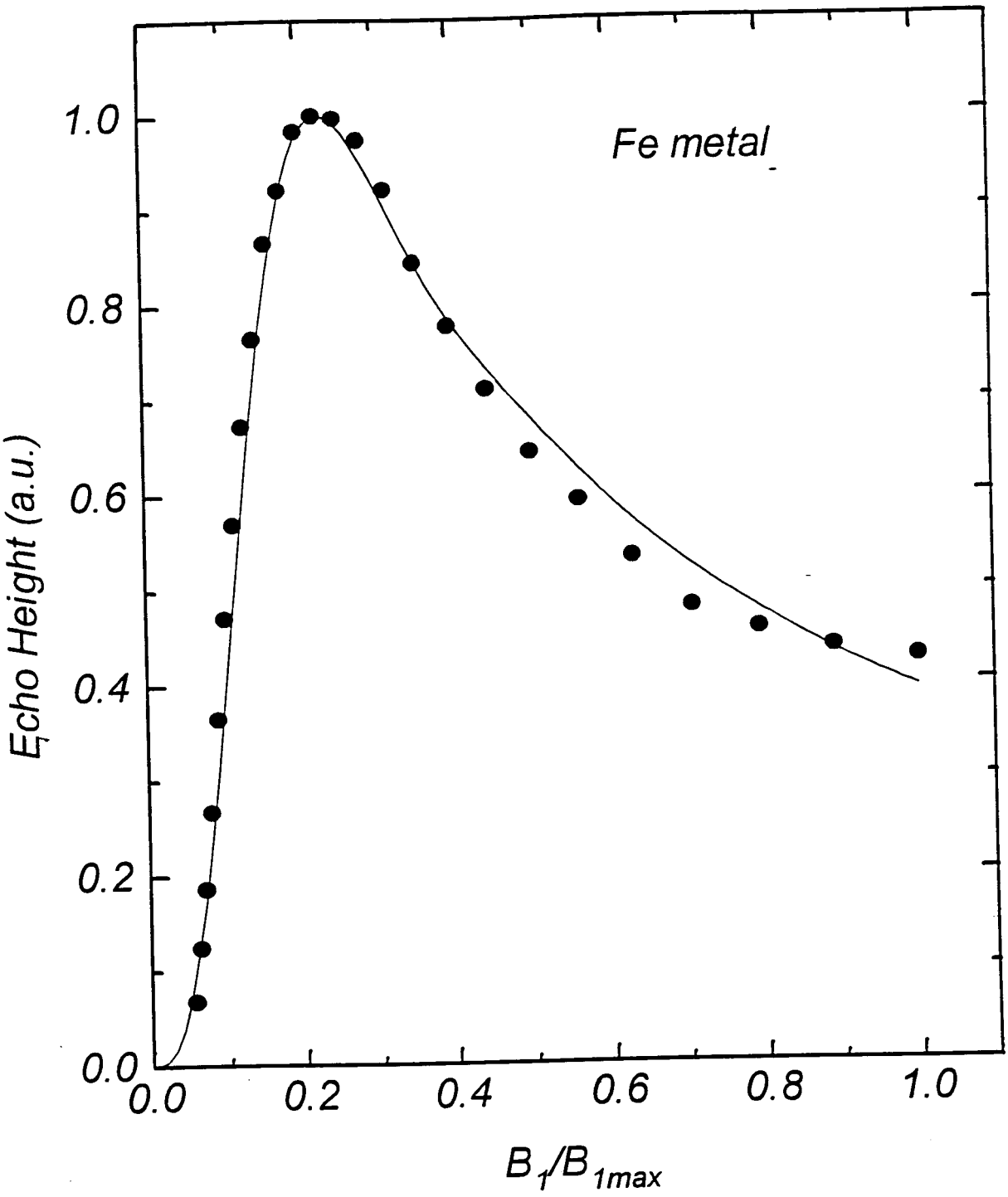

FIG. 1

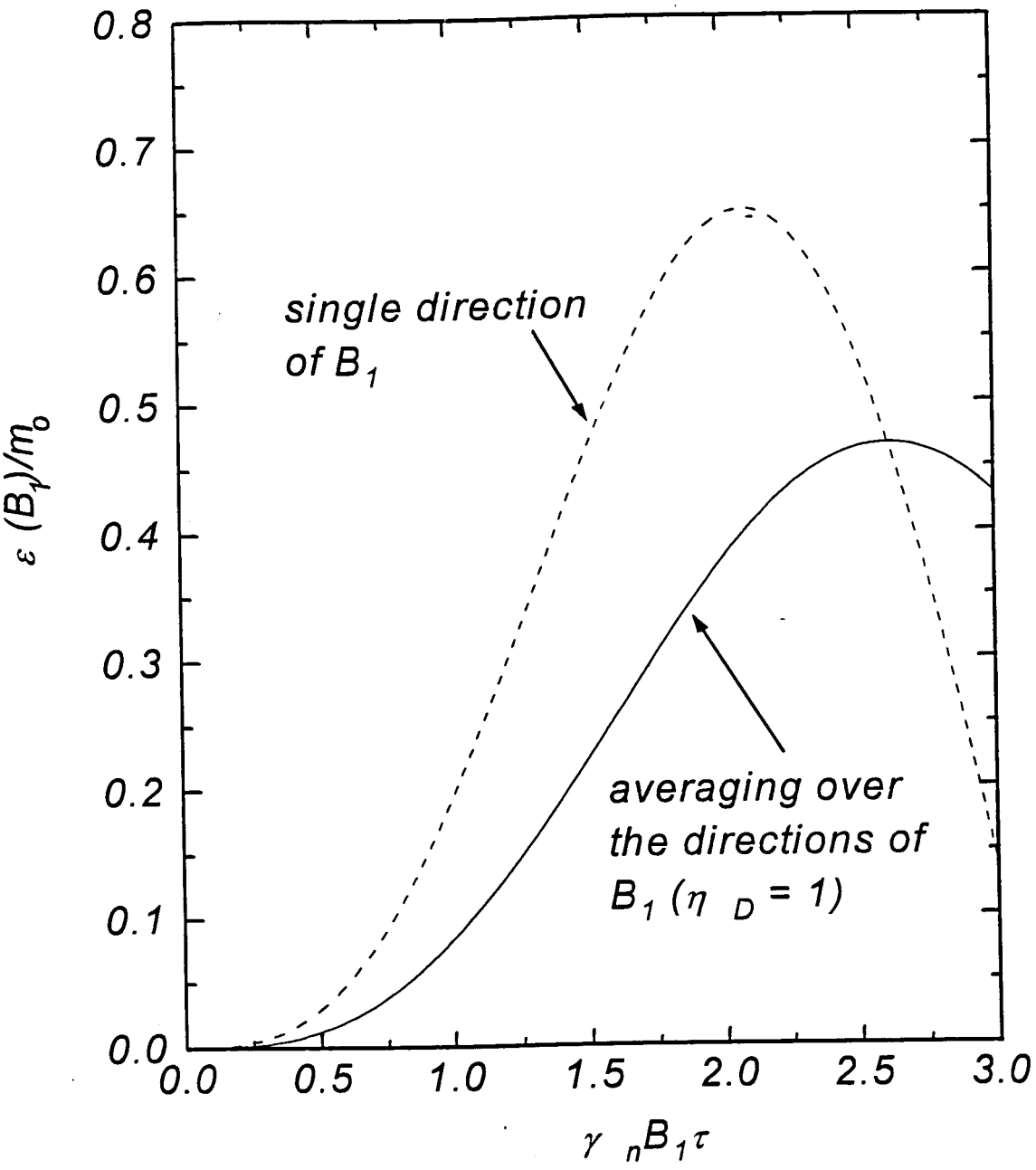
0.8
0.7
0.6
0.5
0.4
0.3
0.2
0.1
0.0
0.0
0.5
1.0
1.5
2.0
2.5
3.0
ε (B1)/m0
γ nB1τ
single direction
of B1
averaging over
the directions of
B1 (η D = 1)

FIG. 2

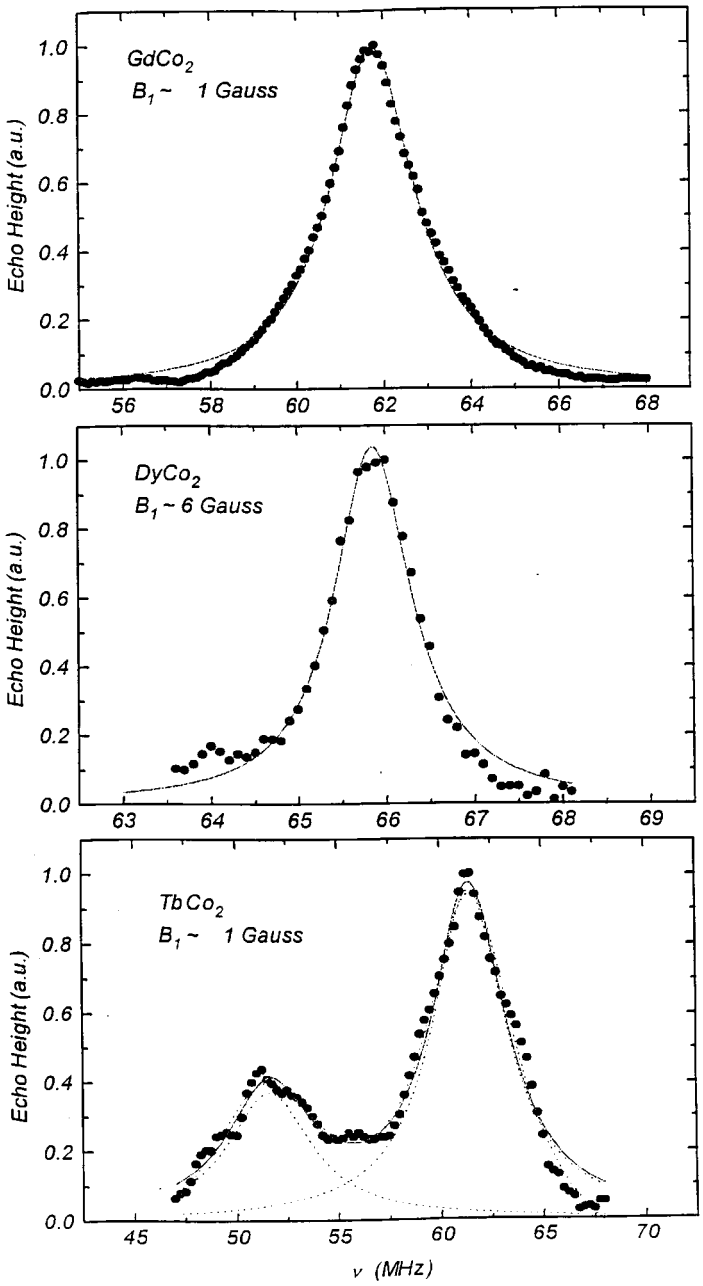
GdCo2
B1 ~ 1 Gauss
DyCo2
B1 ~ 6 Gauss
TbCo2
B1 ~ 1 Gauss
Echo Height (a.u.)
ν (MHz)

FIG. 3

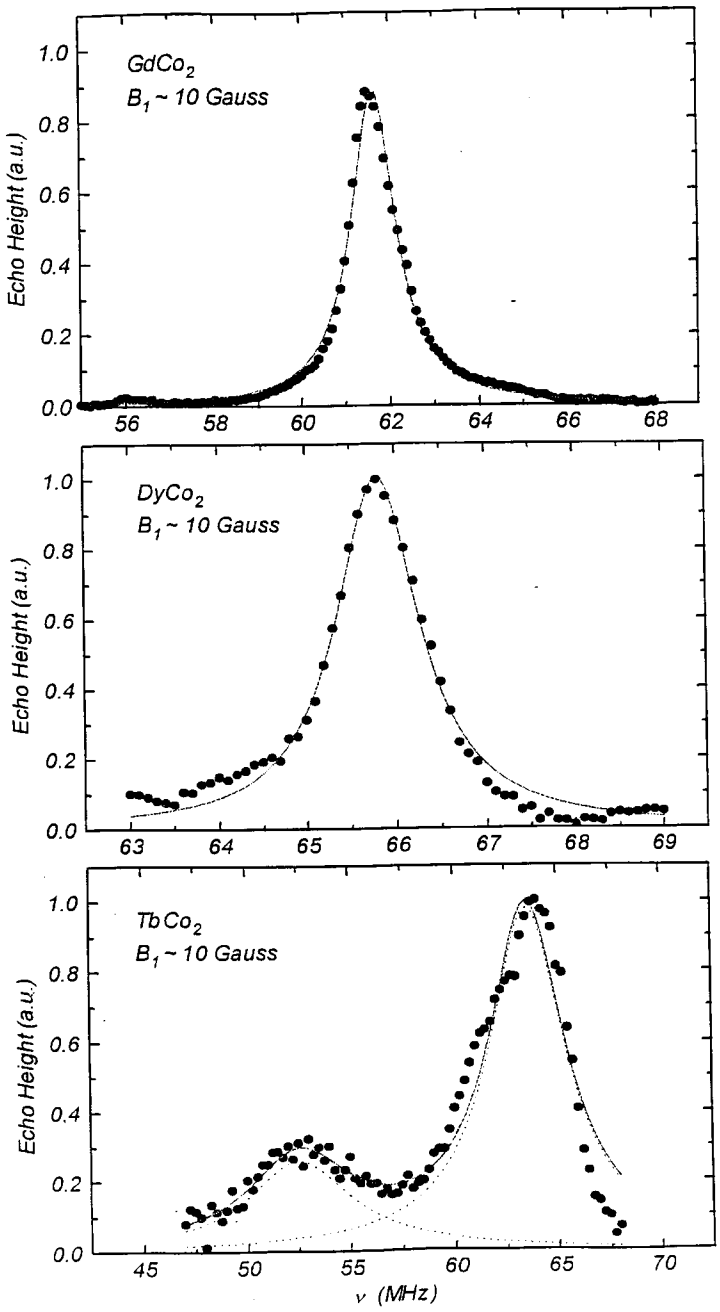
GdCo2
B1 ~ 10 Gauss
DyCo2
B1 ~ 10 Gauss
TbCo2
B1 ~ 10 Gauss
Echo Height (a.u.)
ν (MHz)

FIG. 4

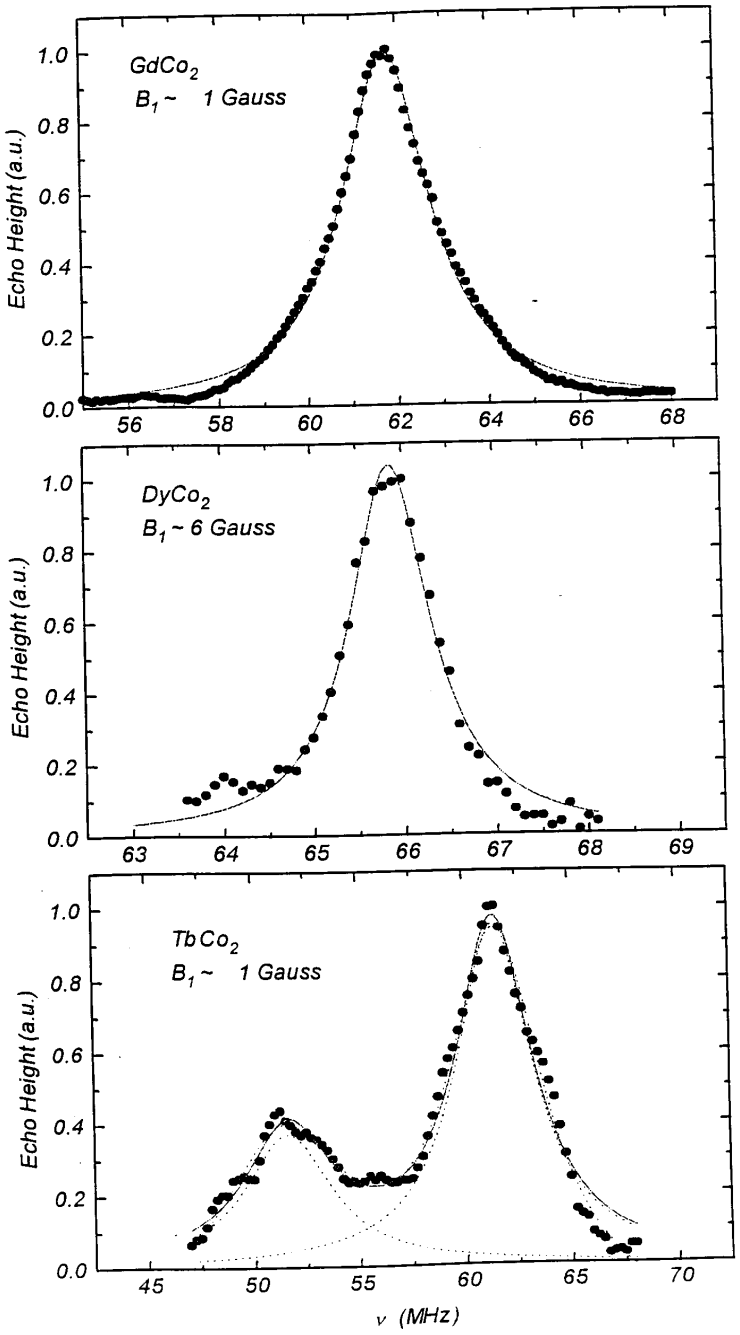
GdCo2
B1 ~ 1 Gauss
DyCo2
B1 ~ 6 Gauss
TbCo2
B1 ~ 1 Gauss
Echo Height (a.u.)
ν (MHz)

FIG. 3

Acknowledgements

The authors wish to express their gratitude to Dr. S.R. Rabbani and Mr. R.S. Sarthour for their suggestions and useful discussion.

References

[1] M.A.H. MacCausland and I.S. Mackenzie, *Nuclear Magnetic Resonance in Rare Earth Metals*, Taylor and Francis, London (1980)

[2] E.A. Turov and M.P. Petrov, *Nuclear Magnetic Resonance in Ferro and Antiferromagnets*, John Wiley and Sons, New York (1966)

[3] C. Kittel and J.K. Galt, *Solid State Physics*, Ed. F.Seitz and D.Turnbull, Academic Press, New York (1956) 437

[4] E. Dormann, *Handbook on Physics and Chemistry of Rare Earths* **14** (1991) 63

[5] E.T. Jaynes, *Phys. Rev.* **98** (1955) 1099

[6] A.L. Bloom, *Phys. Rev.* **98** (1955) 1105

[7] M.B. Stearns, *Phys. Rev.* **162** (1967) 496

[8] G.D. Webber and P.C. Riedi, *J. Phys. Sci. Instr.* **14** (1981) 1159

[9] E. Fukushima and S.B.W.Roeder, *Experimental Pulse NMR: A Nuts and Bolts Approach*, Addison-Wesley, London (1981)

[10] S. Hirosawa and Y.Nakamura, *J. Mag. Mag. Mat.* **25** (1982) 284

[11] M. Bauer and E. Dormann, *Phys. Lett.* A **146** (1990) 55

[12] H. Figiel, *Mag. Mag. Rev.* **16** (1991) 101

[13] T. Dumelow, P.C. Riedi, J.S. Abell and O. Prakash, *J.Phys.F: Met. Phys.* **18** (1988) 77

[14] I.S. Oliveira, *private communication*

[15] D. Kotzur, M. Mehring and O. Kanert, *Z. Naturforch* **28 a** (1973) 1607